Improvements of Myocardial Deformation Assessment by Three-Dimensional Speckle-Tracking versus Two-Dimensional Speckle-Tracking Revealed by Cardiac Magnetic Resonance Tagging

Mihaela S. Amzulescu, MD, Hélène Langet, PhD, Eric Saloux, MD, PhD, Alain Manrique, MD, PhD, Allison Slimani, MD, Pascal Allain, PhD, Clotilde Roy, MD, Christophe de Meester, PhD, Agnès Pasquet, MD, PhD, Oudom Somphone, PhD, Mathieu De Craene, PhD, David Vancraeynest, MD, PhD, Anne-Catherine Pouleur, MD, PhD, Jean-Louis Vanoverschelde, MD, PhD, and Bernhard L. Gerber, MD, PhD, *Brussels, Belgium; and Suresnes and Caen, France*

Background: In prior work, the authors demonstrated that two-dimensional speckle-tracking (2DST) correlated well but systematically overestimated global longitudinal strain (LS) and circumferential strain (CS) compared with two-dimensional cardiac magnetic resonance tagging (2DTagg) and had poor agreement on a segmental basis. Because three-dimensional speckle-tracking (3DST) has recently emerged as a new, more comprehensive evaluation of myocardial deformation, this study was undertaken to evaluate whether it would compare more favorably with 2DTagg than 2DST.

Methods: In a prospective two-center trial, 119 subjects (29 healthy volunteers, 63 patients with left ventricular dysfunction, and 27 patients with left ventricular hypertrophy) underwent 2DST, 3DST, and 2DTagg. Global, regional (basal, mid, and apical), and segmental (18 and 16 segments per patient) LS and CS by 2DST and 3DST were compared with 2DTagg using intraclass correlation coefficients (ICCs) and Bland-Altman analysis. Test-retest reproducibility of 3DST and 2DST was compared in 48 other patients.

Results: Both global LS and CS by 3DST agreed better with 2DTagg (ICC = 0.89 and ICC = 0.83, $P < .001$ for both; bias = 0.5 ± 2.3% and 0.2 ± 3%) than 2DST (ICC = 0.65 and ICC = 0.55, $P < .001$ for both; bias = −5.5 ± 2.5% and −7 ± 5.3%). Unlike 2DST, 3DST did not overestimate deformation at the regional and particularly the apical levels and at the segmental level had lower bias (LS, 0.8 ± 2.8% vs −5.3 ± 2.4%; CS, −0.01 ± 2.8% vs −7 ± 2.8%, respectively) but similar agreement with 2DST (LS: ICC = 0.58 ± 0.16 vs 0.56 ± 0.12; CS: ICC = 0.58 ± 0.12 vs 0.51 ± 0.1) with 2DTagg. Finally, 3DST had similar global LS, but better global CS test-retest variability than 2DST.

Conclusions: Using 2DTagg as reference, 3DST had better agreement and less bias for global and regional LS and CS. At the segmental level, 3DST demonstrated comparable agreement but lower bias versus 2DTagg compared with 2DST. Also, test-retest variability for global CS by 3DST was better than by 2DST. This suggests that 3DST is superior to 2DST for analysis of global and regional myocardial deformation, but further refinement is needed for both 3DST and 2DST at the segmental level. (J Am Soc Echocardiogr 2018;■:■-■.)

Keywords: Speckle-tracking echocardiography, Two-dimensional, Three-dimensional, Magnetic resonance imaging, Strain

From the Division of Cardiology, Department of Cardiovascular Diseases, Cliniques Universitaires St. Luc, Pôle de Recherche Cardiovasculaire, Institut de Recherche Expérimentale et Clinique, Université Catholique de Louvain, Brussels, Belgium (M.S.A., A.S., C.R., C.M., A.P., D.V., A.-C.P., J.-L.V., B.L.G.); Philips Clinical Research Board (H.L.); Philips Research, Medical Imaging (Medisys) (P.A., O.S., M.D.C.), Suresnes; the University Hospital of Caen (E.S.); and EA 4650, Caen University, FHU REMOD-VHF (A.M.), Caen, France.

Grant support was provided by Fondation Nationale de la Recherche Scientifique of the Belgian Government (FRSM PDR 19488731).

Conflicts of Interest: H.L., P.A., and M.D.C. are employed by Philips Medical Systems. Cliniques Universitaires St. Luc have a master research agreement with Philips Medical Systems. The remaining authors reported no actual or potential conflicts of interest.

Reprint requests: Bernhard L. Gerber, MD, PhD, FACC, FESC, FAHA, Division of Cardiology, Department of Cardiovascular Diseases, Cliniques Universitaires St. Luc UCL, Av Hippocrate 10/2806, B-1200 Woluwe St, Lambert, Belgium (E-mail: *bernhard.gerber@uclouvain.be*).

0894-7317/$36.00

https://doi.org/10.1016/j.echo.2018.04.009

Abbreviations

2D = Two-dimensional

2DST = Two-dimensional speckle-tracking

2DTagg = Two-dimensional tagging

3D = Three-dimensional

3DST = Three-dimensional speckle-tracking

CMR = Cardiac magnetic resonance

CS = Circumferential strain

EDV = End-diastolic volume

ESV = End-systolic volume

GCS = Global peak circumferential strain

GLS = Global peak longitudinal strain

ICC = Intraclass correlation coefficient

LS = Longitudinal strain

LV = Left ventricular

Estimation of systolic strain by speckle-tracking echocardiography has become widely popular to quantify myocardial deformation, making it possible to detect subclinical disease[1-3] and obtain prognostic information[4] in various cardiac pathologies. Although the technique has been validated in vitro and in vivo,[5,6] significant dissimilarities between two-dimensional speckle-tracking (2DST) strain measurements performed using different ultrasound machines and different strain software packages have been observed in clinical studies.[7-9] Therefore, efforts to standardize deformation imaging among software packages have been undertaken by the industry at the initiative of a European Association of Cardiovascular Imaging/American Society of Echocardiography task force.[10] In prior work, aiming to validating 2DST against cardiac magnetic resonance (CMR) two-dimensional tagging (2DTagg)–derived strain in a large population of patients,[11] we found a good correlation of global peak longitudinal strain (GLS) and global peak circumferential strain (GCS) among both methods but observed that there was systematic overestimation by 2DST compared with CMR, which was more important for GCS than for GLS. Moreover, on a regional basis, we observed greater heterogeneity of strain in healthy volunteers with 2DST than with 2DTagg and poor agreement between 2DST longitudinal strain (LS) and circumferential strain (CS) and 2DTagg, with important variation among segments.

Three-dimensional speckle-tracking (3DST) derived from three-dimensional (3D) echocardiographic images has recently emerged as a new technique for objectively evaluating myocardial deformation with the potential advantage of assessing complex 3D cardiac structure and function by following speckles in three dimensions over time.[12,13] Although the technique compared favorably with 2DST,[14-16] there have been few comparisons against other imaging methods.[17]

Hence, the aim of this study was two-fold: (1) to investigate the potential advantage of 3DST over 2DST by comparing both techniques with the current standard of two-dimensional (2D) deformation analysis, CMR tagging, in a large group of patients with various heart diseases and (2) to evaluate if 3DST would allow better robustness and less test-retest variability of measurements than 2DST.

METHODS

Study Population

The study protocol was previously published.[11] Briefly, at two sites (Brussels, Belgium, and Caen, France), subjects with various heart diseases and healthy volunteers were prospectively recruited after giving written informed consent to the institutional review board–approved protocol (Comité Ethique Hospitalo Facultaire Université Catholique de Louvain, Brussels, Belgium, and Comité de Protection des Personnes Nord-Ouest III, Caen, France). We screened two patient populations. Healthy volunteers of both sexes and of different ages without any cardiovascular history were recruited by advertisement in the local community. Before inclusion and CMR, all volunteers underwent clinical examinations and assessment of medical history and cardiovascular risk factors, rest and stress electrocardiography, 2D echocardiography, and blood sampling. Exclusion criteria for volunteers were any evidence of heart disease as indicated by clinical history, physical examination, presence of abnormalities on rest or stress electrocardiography, presence of abnormal cardiac function or valve disease on echocardiography, and pregnancy. The patient group included those undergoing clinically indicated CMR for characterization of left ventricular (LV) hypertrophy (hypertrophic cardiomyopathy and aortic stenosis) or LV dysfunction (either ischemic heart disease or nonischemic dilated cardiomyopathy). Exclusion criteria were atrial fibrillation or multiple premature beats and contraindication to CMR (pacemaker or other magnetic resonance–incompatible implant, claustrophobia, severe renal failure). All subjects underwent echocardiography and CMR within 48 hours. In the present study, we studied a subset of 119 of our initial 139 recruited patients, in whom we performed 3D echocardiographic examinations of sufficient quality to allow 3DST analysis.

Two-Dimensional and 3D Echocardiography

Echocardiography was performed using an iE33 and Epic ultrasound system (Philips Medical Systems, Andover, MA) equipped with a 1- to 5-MHz transthoracic matrix-array transducer (xMATRIX X5.1) with both 2D and 3D capabilities. Two-dimensional grayscale harmonic images were acquired in the apical views (two, three, and four chamber) and the short-axis views (at the basal, mid, and apical ventricular levels) at a frame rate of 55 to 60 frames/sec during breath-hold, as previously described.[11] Care was taken to avoid foreshortening in apical views and to image the true apex in short-axis views. Thereafter, a 3D full volume was acquired from the apical view, with minimum depth to encompass the entire left ventricle, in apnea during four consecutive heartbeats with temporal resolution of 22 to 25 frames/sec.

All 2D and 3D images were saved in Philips's "native" Digital Imaging and Communications in Medicine format (which contains additional tags with information on high-integrity acoustic information stored in a data-rich format akin to raw), transferred to an Xcelera version 2.1 picture archiving and communication system server. Speckle-tracking analysis of the "native" data was performed offline by a single observer. The time required to perform the 2DST and 3DST analyses was documented. Two-dimensional images were analyzed using aCMQ software (QLAB version 10.3, Philips Medical Systems), as previously described.[11] Briefly, global and segmental longitudinal and circumferential peak systolic Lagrangian 2DST strain values were computed on the basis of 18- and 16-segment models, respectively. The measured deformation for each segment was a weighted combination of the local displacements, with a greater weight given to the endocardium than to the epicardium. The strain waveform was calculated from the per-region deformation at the endocardial border. The global strain waveform was derived as a weighted average of the segmental waveforms. Three-dimensional images were analyzed using prototype software (Philips Research, Medisys, Suresnes, France) on the basis of Sparse Demons motion estimation.[18] An optimal dense, nonrigid displacement field

HIGHLIGHTS

- 3DST GLS and GCS agreed better with 2DTagg than 2DST.
- Unlike 2DST, 3DST did not overestimate GCS vs 2DTagg.
- Segmental strains by both 3DSTand 2DST agreed suboptimally with 2DTagg.
- 3DST and 2DST test-retest reproducibility were similar for GLS. 3DST had better GCS test-retest reproducibility than 2DST.

was computed between contiguous frames by minimizing an energy defined only on a finite number of points of interest in the LV segmentation. Multilayer LV segmentation was initialized in end-diastole by using the same automated segmentation algorithm that is used for Philips HeartModel[19]: end-diastole was determined by detection of the electrocardiographic R-wave peak time, LV long-axis orientation was then estimated, and an adaptive algorithm generated a LV mesh on the basis of a priori knowledge gained from training on an LV atlas of various LV morphologies. When necessary, the endocardial border could be further refined by the operator, either globally or locally. For the majority of our patients, we performed both global and local editing, to ensure correct tracking and therefore accurate strain information. A screen-capture video showing the step-by-step analysis of a 3D full-volume data set is available (Video 1 available at www.onlinejase.com). Transmural segmental and global strain waveforms were calculated from length change along the longitudinal and circumferential directions in the LV meshes that were deformed by the estimated displacement field. As for 2D imaging, global and segmental longitudinal and circumferential peak systolic Lagrangian 3DST strains were computed on the basis of 18- and 16-segment models, respectively.

Cardiac Magnetic Resonance

CMR studies were acquired using a 3.0-T system (Achieva, Philips Medical Systems) at the two sites (Saint Luc Hospital, Brussels, Belgium, and GIP CYCERON, Caen, France), as previously described.[11] We first acquired one set of conventional 1-cm-thick retrospectively gated steady-state free precession short-axis slices covering the left ventricle and two-, three-, and four-chamber long-axis slices, respectively. To study myocardial deformation, we repeated acquisition of eight to 10 short-axis and three long-axis images using prospectively triggered cine hybrid gradient-echo sequences with echoplanar readout and grid spatial modulation of magnetization tagging in identical prescriptions. Parameters were as follows: field of view, 36 to 40 cm; slice thickness, 8 to 10 mm; repetition time, 7.2 msec; echo time, 2.0 to 4.2 msec; flip angle, 12°; echoplanar factor, 7; matrix size, 256 × 96 to 140; temporal resolution, 20 to 40 msec; and tag spacing, 7 mm.

Short-axis steady-state free precession cine images were analyzed using Segment version 1.9 (Medviso, Lund, Sweden) to compute LV volumes, mass, and ejection fraction as previously described. Tagged images were analyzed using HARP software (Diagnosoft

Table 1 Baseline and CMR characteristics of patients and volunteers

	Volunteers (n = 29)	Dysfunction (n = 63)	Hypertrophy (n = 27)	P
Age (y)	49 ± 17	54 ± 16	57 ± 16	.24
Men	15 (52)	52 (83)§	21 (78)	.006
Weight (kg)	71 ± 11	74 ± 13	73 ± 12	.56
Height (cm)	171 ± 8	173 ± 7	170 ± 7	.28
BSA (m^2)	1.8 ± 0.2	1.9 ± 0.2	1.9 ± 0.2	.42
SBP (mm Hg)				
Echocardiography	128 ± 22	120 ± 23	122 ± 19	.44
CMR	130 ± 20	125 ± 18	133 ± 19	.57
DBP (mm Hg)				
Echocardiography	79 ± 12	75 ± 15	72 ± 11	.32
CMR	79 ± 12	80 ± 12	73 ± 8	.74
HR (beats/min)				
Echocardiography	63 ± 10	70 ± 19	67 ± 11	.14
CMR	63 ± 9	72 ± 16§	68 ± 11	.01
CMR data				
LV EDVi (mL/m^2)	87 ± 16	144 ± 45*	88 ± 20	.0001
LV ESVi (mL/m^2)	32 ± 8	102 ± 48*	29 ± 12	.0001
LVEF (%)	64 ± 5	31 ± 13*	68 ± 9	.0001
LV mass index (g/m^2)	56 ± 9†	77 ± 18	94 ± 37‡	.0001

BSA, Body surface area; *DBP*, diastolic blood pressure; *EDVi*, indexed end-diastolic volume; *ESVi*, indexed end-systolic volume; *HR*, heart rate; *LVEF*, LV ejection fraction; *SBP*, systolic blood pressure.
Data are expressed as mean ± SD or as number (percentage).
*P < .0001 versus volunteers and hypertrophy.
†P < .003 versus dysfunction and hypertrophy.
‡P < .01 versus dysfunction.
§P < .005 versus volunteers.

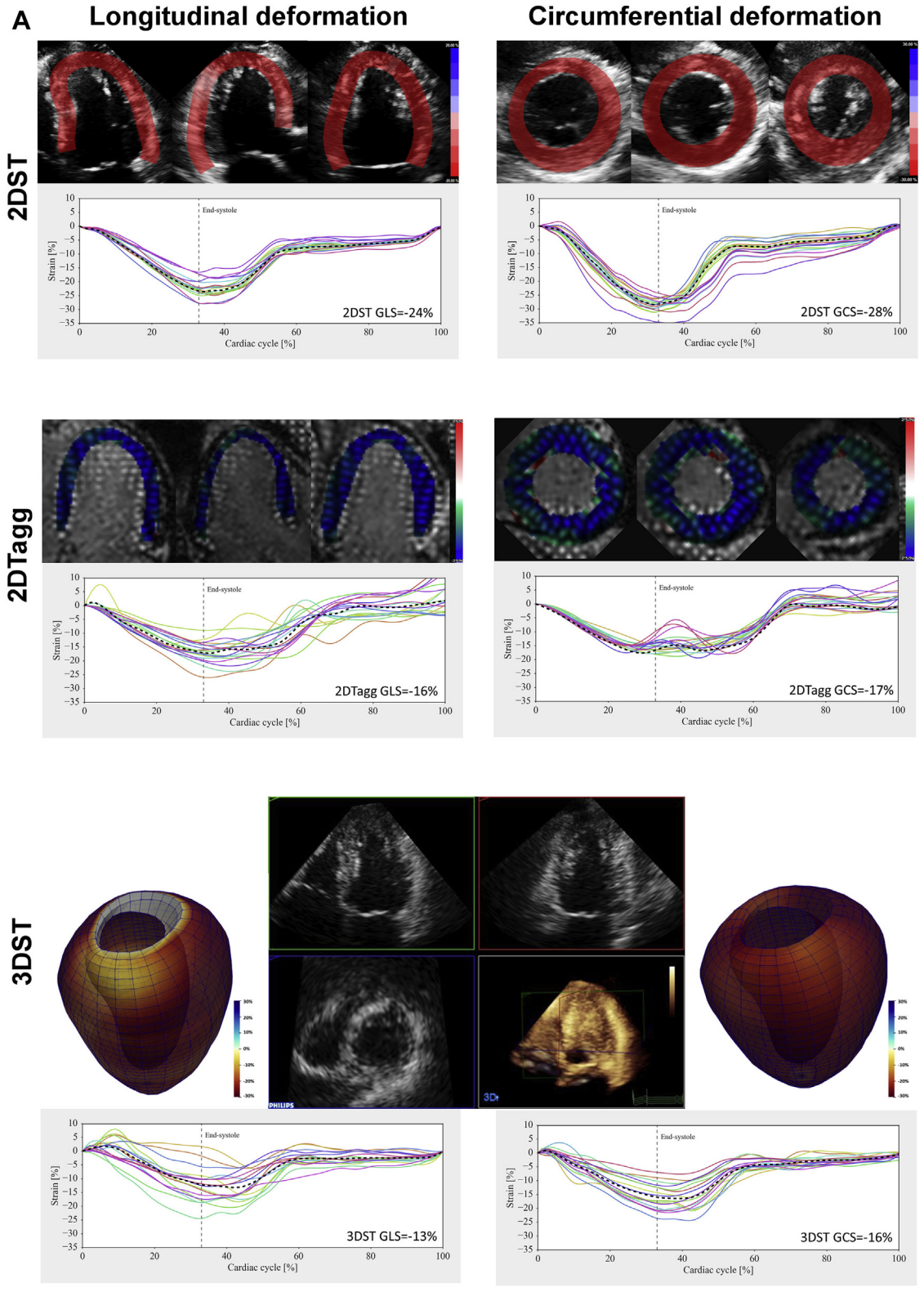

Figure 1 Representative 2DST, 3DST, and 2DTagg images and associated strain curves from a healthy volunteer **(A)** and a patient with LV dysfunction **(B)**. All LV views are end-systolic frames with color-coded strain values superimposed on 2DST and 2DTagg images. Color scale differs for each modality.

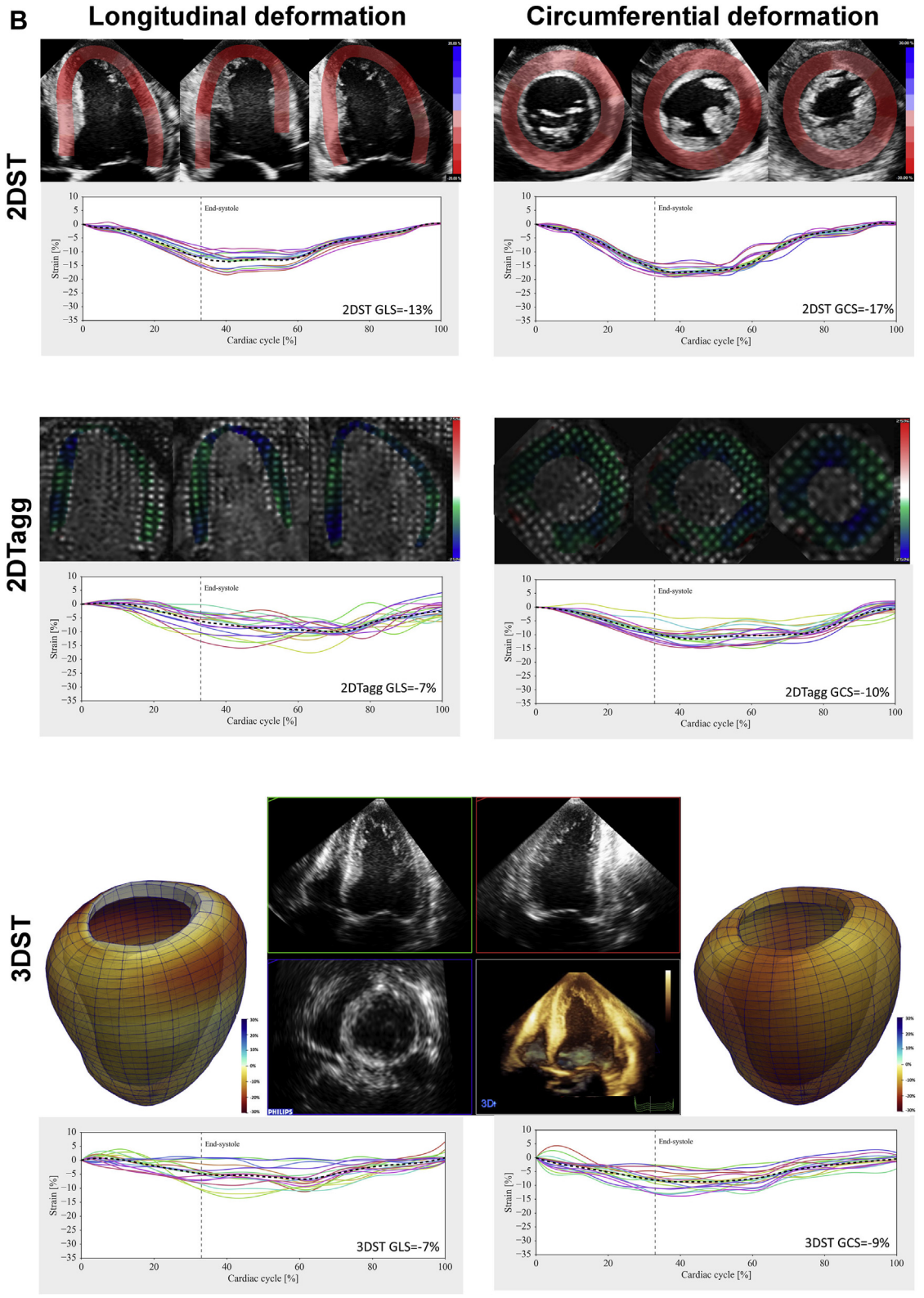

Figure 1 (*continued*).

version 2.7; Diagnosoft, Baltimore, MD), and segmental Lagrangian longitudinal and circumferential peak systolic strains were computed on the basis of 18- and 16-segment models, respectively. The waveforms were filtered to remove large outliers and extended in end-diastole using gradient extrapolation to compensate for the delayed acquisition of the first phase (about 30 msec after detection of the electrocardiographic R-wave peak time). The global strain waveform was derived as a weighted average of the segmental waveforms; that

Table 2 Normal GLS by 2DST, 3DST, and 2DTagg in healthy volunteers

	2DST	3DST	2DTagg
GLS (%)	−21 ± 2*	−14 ± 2†	−15 ± 2
GCS (%)	−26 ± 4*	−15 ± 2	−16 ± 2

Data are expressed as mean ± SD.
*P < .0001 versus 2DTagg.
†P = .03 versus 2DTagg.

is, instead of each of the segmental waveforms contributing equally to the global strain waveform, some segments contributed more than others to account for differences in segment lengths. The time needed to perform the 2DTagg analysis was also recorded.

Test-Retest Echocardiography

Test-retest reproducibility of 2DST and 3DST was evaluated in a second population of 48 consecutive patients with various pathologies undergoing echocardiography for clinical reasons in the echocardiography laboratory of Cliniques Universitaires Saint Luc. Two-dimensional and 3D acquisitions performed as described earlier were acquired with an approximately 10-min interval, first by echocardiography technicians with >5 years of experience and then by a single certified transthoracic echocardiographic physician blinded to the initial image acquisition. The test-retest analysis was done by a single trained observer, and measurements of matching echocardiographic data sets were performed with a 1-week interval from each other.

Statistical Analysis

Statistical analysis was performed using SPSS version 21.0 (SPSS, Chicago, IL). P values < .05 were considered to indicate statistical significance. Continuous variables are presented as mean ± SD and categorical variables as counts and percentages. One-way analysis of variance with Bonferroni (for normal distribution) or Games-Howell (for unequal variances) post hoc correction was used to compare baseline and CMR characteristics of subjects. Intertechnique comparisons were performed using linear Pearson correlation, two-way mixed intraclass correlation coefficients (ICCs), and the Bland-Altman method of estimation of bias, at the segmental (18 segments per patient for LS and 16 segments per patient for CS), regional (base, mid, and apical), and global LV levels. Test-retest reproducibility of strain measurements was assessed at the global and segmental levels using the Bland-Altman method and two-way mixed ICCs.

RESULTS

Clinical and CMR Characteristics of Patients

Baseline characteristics of the study population are presented in Table 1. For the entire study population, systolic and diastolic blood pressure was significantly lower at the time of echocardiography than in the magnetic resonance environment (121 ± 22 vs 129 ± 19 mm Hg [P = .02] and 75 ± 15 vs 80 ± 11 mm Hg [P = .03], respectively), while heart rate was similar (67 ± 15 vs 68 ± 14 beats/min, P > .05). Patients with LV dysfunction had the largest indexed LV volumes and lowest ejection fractions. LV indexed mass was lowest in volunteers and highest in the LV hypertrophy group. The average analysis times for 2DTagg (9–11 min) and 2DST (7–9 min) were considerably longer than for 3DST (3–5 min). Representative images and strain curves from a healthy volunteer and a patient with LV dysfunction are shown in Figure 1 and Videos 2–5 (available at www.onlinejase.com).

Normal Global and Regional LS and CS in Healthy Volunteers

Normal global strain values in the 29 healthy volunteers are shown in Table 2. Normal GLS was significantly higher by 2DST and slightly lower by 3DST versus 2DTagg (−21 ± 2% and −14 ± 2% vs −15 ± 2% for GLS, P < .0001 and P < .03, respectively). Normal GCS was significantly higher by 2DST than by 3DST compared with 2DTagg (−26 ± 4% and −15 ± 2% vs −16 ± 2%, P < .0001 and P > .05, respectively).

Bull's-eye plots showing the average and SD of normal regional LS and CS in healthy volunteers by 2DST, 3DST, and 2DTagg are shown in Figure 2. Regional normal LS and CS were variable among LV levels by all modalities. However, by 2DST, LS and CS were significantly higher in the apical than mid and basal segments (−25 ± 2% vs −20 ± 3% and −19 ± 2% for LS and −31 ± 6% vs −26 ± 4% and −24 ± 4% for CS, respectively, P < .0001 for all). By contrast, 3DST was more homogeneous at the different LV levels, with no significant difference for LS (−14 ± 3%, −14 ± 3%, −14 ± 2%, P > .05) but lower values at the LV base compared with mid and apex for CS (−14 ± 3% vs −16 ± 3%, −17 ± 2%, P = .001). This was also true for 2DTagg, for which apex-to-base differences were much less pronounced than for 2DST.

Comparison of GLS and GCS by 2DST and 3DST versus 2DTagg

GLS by both 2DST and 3DST was significantly different in patients with hypertrophy than volunteers (P < .001 for both), while GCS detected differences only by 2DST (P < .001), not by 3DST (P = NS). All methods differentiated patients with dysfunction from volunteers and hypertrophic (P < .01 for all). Global strain by group is described in the Supplemental Table 1 (available at www.onlinejase.com).

Scatterplots and Bland-Altman graphs comparing global strain in the entire population of 119 subjects are shown in Figure 3. For both GLS and GCS, the agreement between 3DST and 2DTagg (ICC = 0.89 and ICC = 0.83, P < .0001 for both) was better than for 2DST versus 2DTagg (ICC = 0.65 and ICC = 0.55, P < .0001 for both). Although 2DST GLS and GCS values were systematically higher (bias = −5.5 ± 2.5% and −7 ± 5.3%) compared with 2DTagg, 3DST GLS and GCS values were not significantly different from 2DTagg (bias = 0.5 ± 2.3% and 0.2 ± 3%). Additionally, as shown in Figure 3, for GCS by 2DST, the slope of the intercept was steep and the bias was skewed, with the highest overestimation being present in the range of normal deformation values. The slope of the intercept was closer to the identity line, and the bias was more homogenously distributed for GCS by 3DST.

Regional and Segmental Strain

As shown in Figure 4A, also at the regional levels, LS by 3DST agreed better with 2DTagg than 2DST, in particular at the apical level (base: ICC = 0.68 vs ICC = 0.59; mid: ICC = 0.85 vs ICC = 0.76; apex: ICC = 0.81 vs ICC = 0.57; P < .0001 for all). At all the LV levels, LS by 3DST had lower biases than by 2DST and did not overestimate deformation, specifically at the apical level (bias −1.1 ± 3.5%, 1.7 ± 2.8%, and 1.1 ± 3.4% for 3DST at the base, mid, and apex;

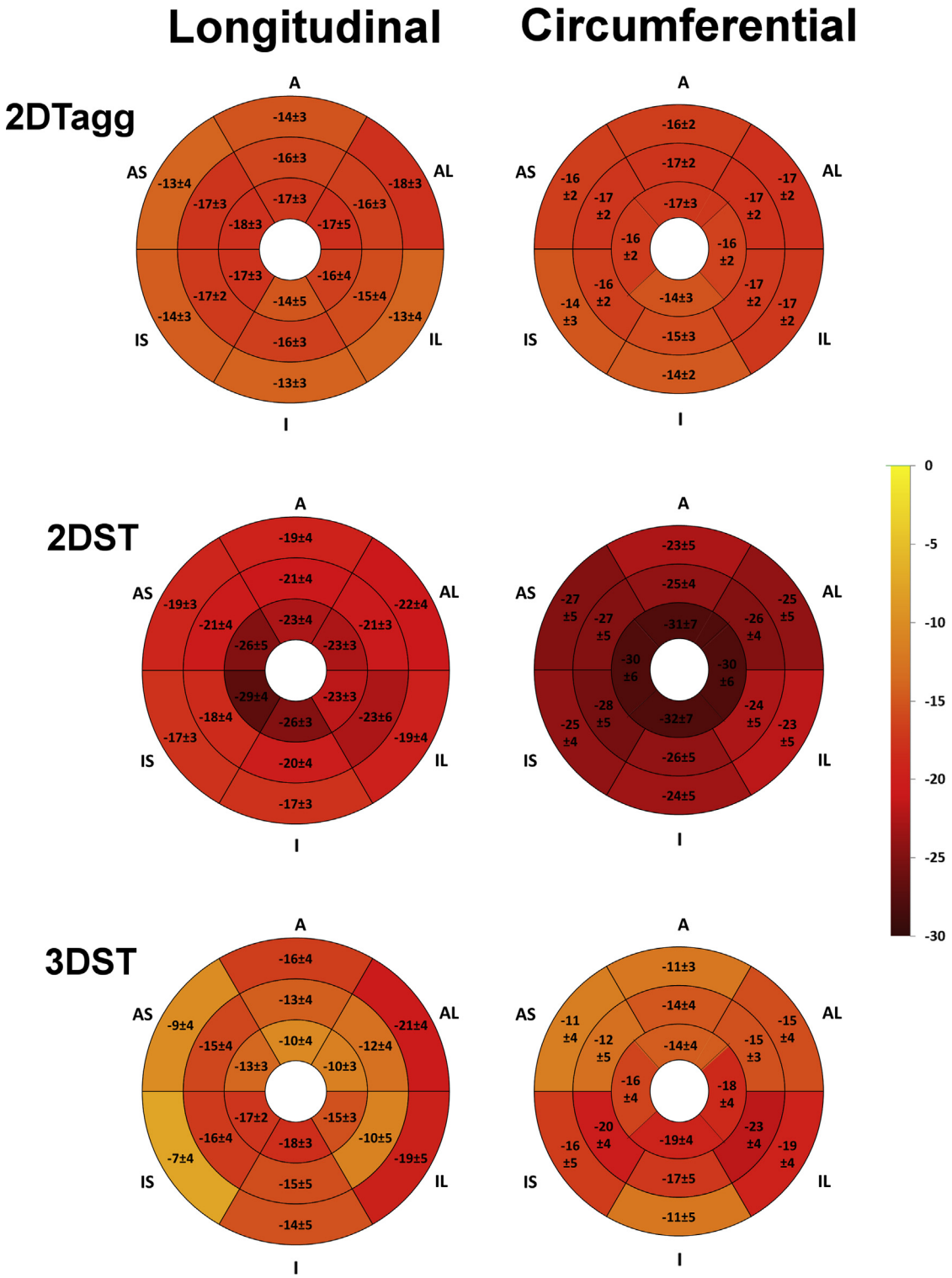

Figure 2 Bull's-eye representations of mean longitudinal and circumferential segmental strain values in healthy volunteers by 2DST, 3DST, and 2DTagg. *A*, Anterior; *AL*, anterolateral; *AS*, anteroseptal; *I*, inferior; *IL*, inferolateral; *IS*, inferoseptal.

bias = −4.4 ± 3.1%, −4.4 ± 2.7%, and −8 ± 3.3% for 2DST at the base, mid, and apex).

The agreement between 3DST and 2DTagg for CS at the different LV levels was better than between 2DST and 2DTagg (base: ICC = 0.80 vs ICC = 0.63; mid: ICC = 0.81 vs ICC = 0.58; apex: ICC = 0.63 vs ICC = 0.36; $P < .0001$ for all; see Figure 4B). Unlike 2DST, which showed increased and skewed biases from base to apex (bias = −5.4 ± 5%, −6.3 ± 6%, and −11 ± 9.2%), bias was lower and more homogenously distributed with 3DST (bias = 1.3 ± 2.9%, −0.6 ± 3.6%, and −1.4 ± 5.2%).

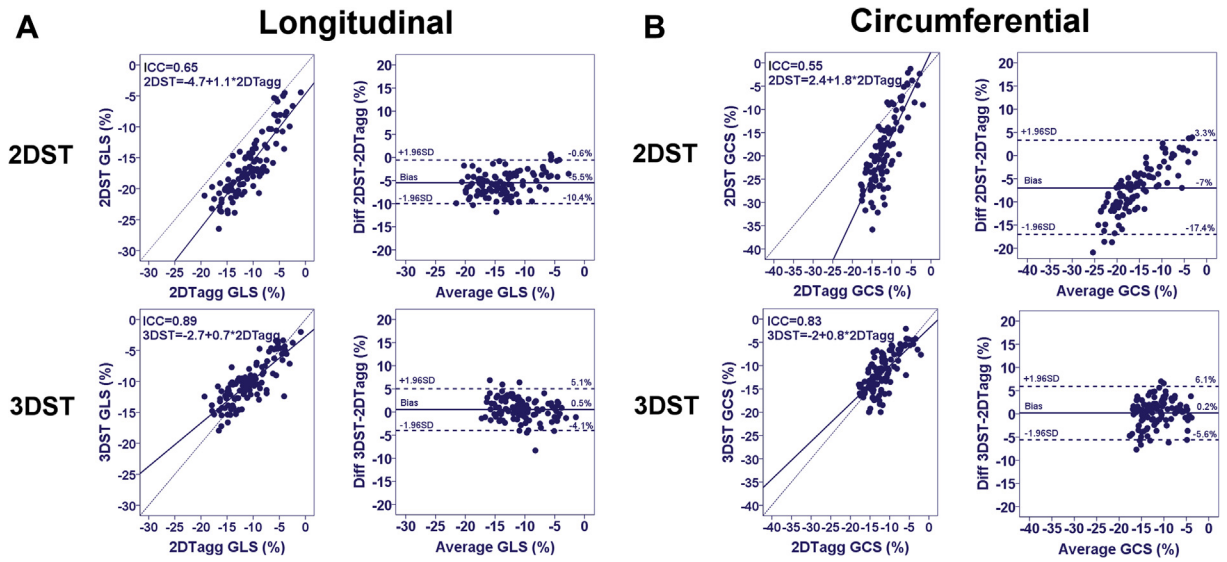

Figure 3 Scatterplot and Bland-Altman plot comparing 2DST, 3DST, and 2DTagg. **(A)** Longitudinal strain. **(B)** Circumferential strain.

As shown in Figure 5, in the entire population, 3DST had lower segmental strain values than 2DST, particularly at the apical level, for both LS and CS. At the segmental level, 3DST versus 2DTagg had a similar mean ICC to that of 2DST versus 2DTagg (LS: ICC = 0.58 ± 0.16 vs 0.56 ± 0.12; CS: ICC = 0.58 ± 0.12 vs 0.51 ± 0.1) but much lower bias (LS: bias = 0.8 ± 2.8% vs −5.3 ± 2.4%; CS: bias = −0.01 ± 2.8% vs −7 ± 2.8%, respectively).

Test-Retest Reproducibility of 2DST and 3DST

Characteristics of the test-retest population are shown in Table 3. The test-retest variability for GLS and GCS is shown in Table 4. The reproducibility of GLS was similar by 2DST and 3DST (ICC = 0.92 and ICC = 0.82), while GCS was more reproducible by 3DST than by 2DST (ICC = 0.88 and ICC = 0.76; see Figure 6). At segmental level, as shown by the Figure 7, agreement was better by 3DST than by 2DST for CS (mean ICC = 0.73 ± 0.1 vs 0.51 ± 0.1), while it was similar for LS (mean ICC = 0.73 ± 0.1 vs 0.73 ± 0.1).

DISCUSSION

In this study, we compared 3DST and 2DST versus 2DTagg for global, regional, and segmental LV deformation quantification in a large group of patients with various cardiac pathologies. The main findings of our work are as follows.

1. GLS and GCS measurements by 3DST agreed better with 2DTagg than 2DST, and unlike 2DST, 3DST did not overestimate myocardial deformation, especially in the circumferential direction.
2. Compared with 2DTagg, 3DST regional deformation performed better than 2DST, with lower and more homogenously distributed biases, especially for the circumferential regional strain and notably at the apical level.
3. However, at the segmental level, agreement of both 3DST and 2DST with 2DTagg was suboptimal, although with lower biases for 3DST than 2DST.
4. The test-retest reproducibility of 3DST was comparable with that of 2DST for longitudinal deformation but significantly better for the CS.

To our knowledge this is the first study comparing 3DST-derived strain measurements with the current 2D gold standard of myocardial deformation, CMR tagging, while investigating the potential benefits of 3DST over the 2DST technique.

In agreement with previous studies,[14,15] our results show that different values of myocardial deformation are obtained by 3DST than by 2DST, and additionally, we demonstrate that the LS and CS values obtained with 3DST compared more favorably with 2DTagg than values derived from 2DST. While 2DST resulted in systematic strain overestimation, especially in the circumferential direction, this bias was no longer present with 3DST. This finding is reinforced by the regional deformation analysis of the different LV levels showing that 3DST is more stable at the base, mid, and apical levels than 2DST, for longitudinal and, more so, circumferential assessment.

Unquestionably, part of the observed differences between 3DST and 2DST are related to LV twisting and motion of the base of the heart toward the apex, responsible for the through-plane motion of speckles not accounted for by 2DST techniques. Moreover, with 3D acquisition, the entire left ventricle is encompassed in the full-volume data set, overcoming any foreshortening in the long axis and any apical plane misalignment in short axis by 2D imaging, potentially explaining the overestimation of LS and CS, especially at the apical level. Although it is reassuring that 3DST compares well with the gold-standard method of strain quantification, 2DTagg, it would appear to challenge the hypothesis of out-of-plane motion of speckles. However, the observed differences between the techniques should be interpreted taking also into account that different segmentation and tracking algorithms are implemented in the analysis software packages. As described in our prior work, the 2DST algorithm favors the endocardial LV layer, where deformation is higher than in the mid and epicardial LV layers, while with 2DTagg, more transmural information is obtained by tracking taglines within the myocardium. As for the 3DST prototype, it yields transmural strain by estimating the displacement of the speckle pattern within an automated segmentation of the left ventricle by an adaptive model trained on 3D echocardiographic images.

Despite the good results obtained at the global and regional levels, deformation analysis at the segmental level remains challenging for both 3DST and 2DST, although 3DST seems to perform slightly better than 2DST when both are compared with 2DTagg. Whether this results from the difficulty of matching LV segments throughout different imaging techniques or simply the software's

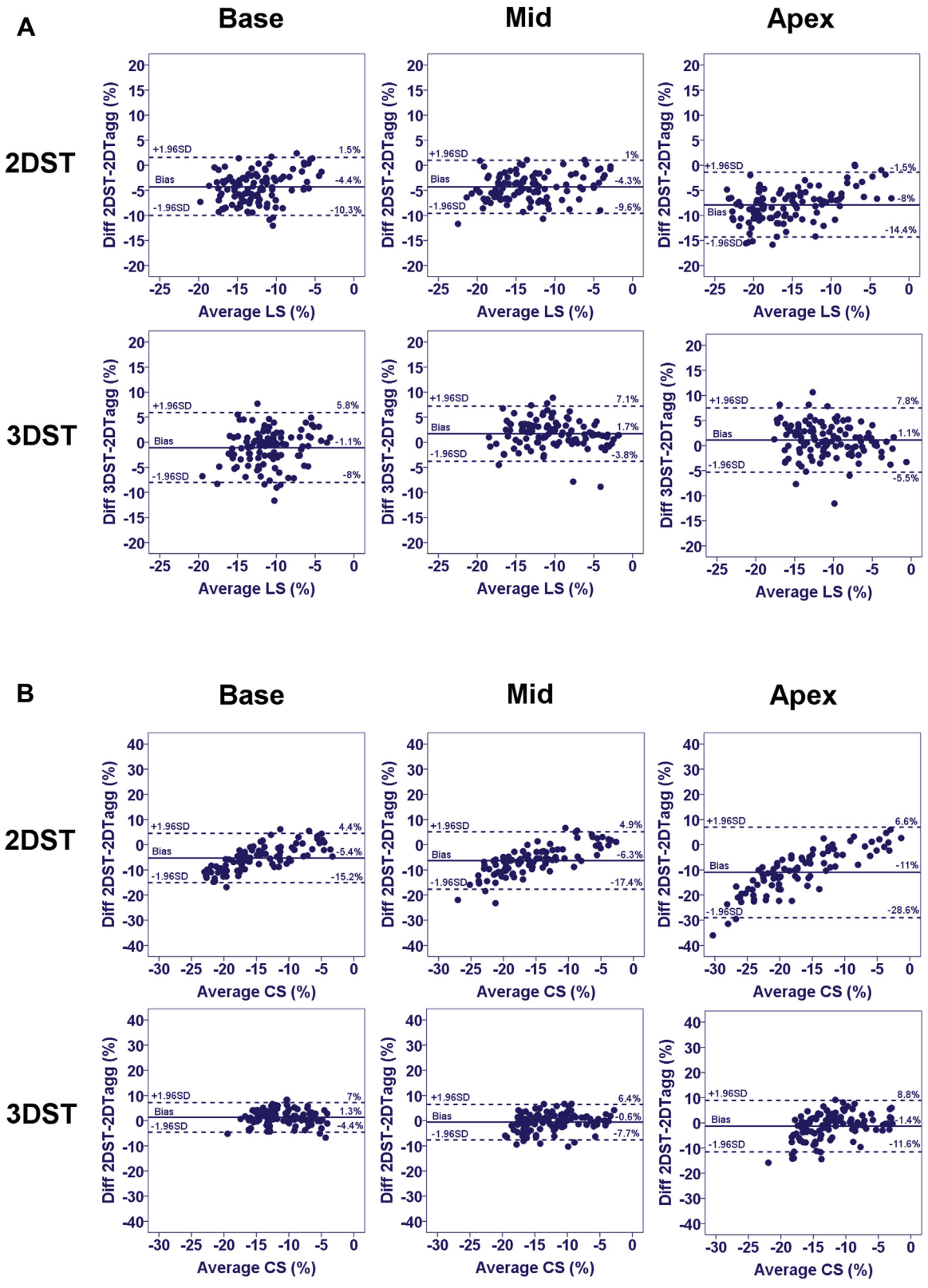

Figure 4 Bland-Altman plots comparing regional strain by level (basal, mid, and apical level) by 2DST and 3DST versus 2DTagg. **(A)** Longitudinal strain. **(B)** Circumferential strain.

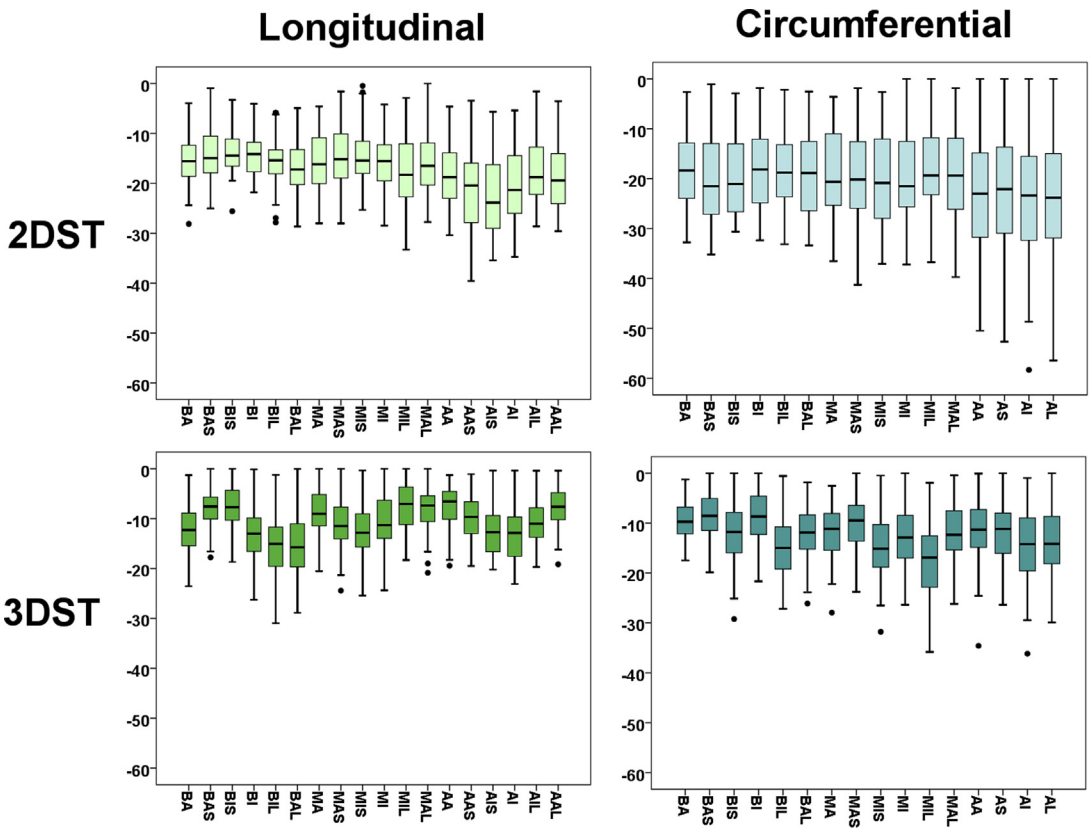

Figure 5 Boxplot graphs showing segmental LS and CS by 2DST and 3DST in the overall population. The boxes represent median and 25th to 75th percentiles, and the whiskers represent the 95% CI. *AA*, Apical anterior; *AAL*, apical anterolateral; *AAS*, apical anteroseptal, *AI*, apical inferior; *AIL*, apical inferolateral; *AIS* apical inferoseptal; *AL*, apical lateral; *AS*, apical septal; *BA*, basal anterior; *BAL*, basal anterolateral; *BAS*, basal anteroseptal; *BI*, basal inferior; *BIL*, basal inferolateral; *BIS* basal inferoseptal; *MA*, mid anterior; *MAL*, mid anterolateral; *MAS*, mid anteroseptal; *MI*, mid inferior; *MIL*, mid inferolateral; *MIS*, mid inferoseptal.

Table 3 Characteristics of the test-retest population ($N = 48$)

Variable	Value
Age (y)	58 ± 16
Men	29 (60)
BSA (m^2)	1.89 ± 0.2
Cardiac pathology	
Normal	27 (56)
LV dysfunction	6 (13)
LV hypertrophy	1 (1)
Valve disease	10 (21)
Other	4 (9)
SBP (mm Hg)	126 ± 20
DBP (mm Hg)	74 ± 12
HR (beats/min)	68 ± 12

BSA, Body surface area; *DBP*, diastolic blood pressure; *HR*, heart rate; *SBP*, systolic blood pressure.
Data are expressed as mean ± SD or as number (percentage).

Table 4 Test-retest reproducibility of global strain measures

Measure	ICC	Mean bias (95% CI)
GLS 2DST	0.92	−0.05 ± 1.9% (−3.7% to 3.6%)
GCS 2DST	0.76	−0.05 ± 3.6% (−7.1% to 7%)
GLS 3DST	0.82	−0.11 ± 2.3% (−4.7% to 4.5%)
GCS 3DST	0.88	0.01 ± 2.2% (−4.4% to 4.4%)

immaturity to accurately depict deformation at a smaller level is a matter of debate. Both 3DST and 2DST have been independently validated versus sonomicrometry in animal models[5,20,21] for the quantification of regional deformation, but when translated to humans, discrepancies appear. The challenge of quantifying segmental strain is becoming a problem increasingly recognized in recent publications as well,[22] which documented significant differences between vendors in the accuracy to identify regional abnormalities.

Yet another argument rendering data interpretation difficult is the inhomogeneous distribution of segmental strain values in the normal population, with 2DST showing systematically higher values in the apical segments, while with 3DST this nonuniformity persisted but did not favor any of the LV levels. Our findings are consistent with those of other studies reporting large dispersion of normal 3D strain segmental values in large group of volunteers,[23] which may be a factor limiting comparison with diseased segments in patients with localized wall involvement. The average longitudinal and circumferential normal strain values by 3DST with the prototype we analyzed were

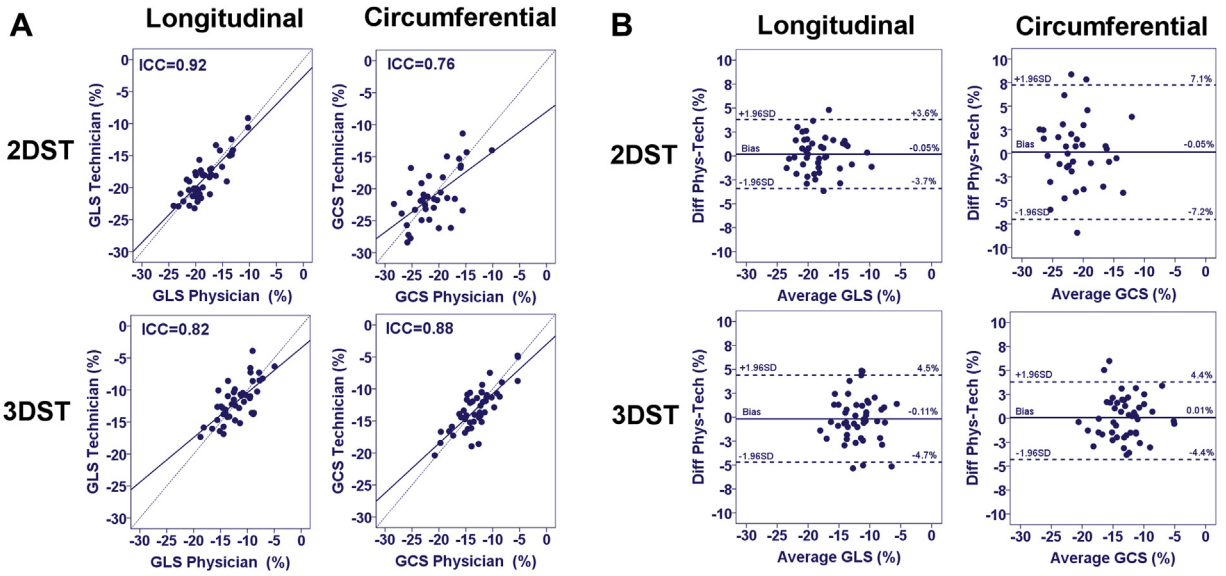

Figure 6 Test-rest reproducibility of GLS and GCS by 2DST and 3DST. **(A)** Scatterplots. **(B)** Bland-Altman graphs.

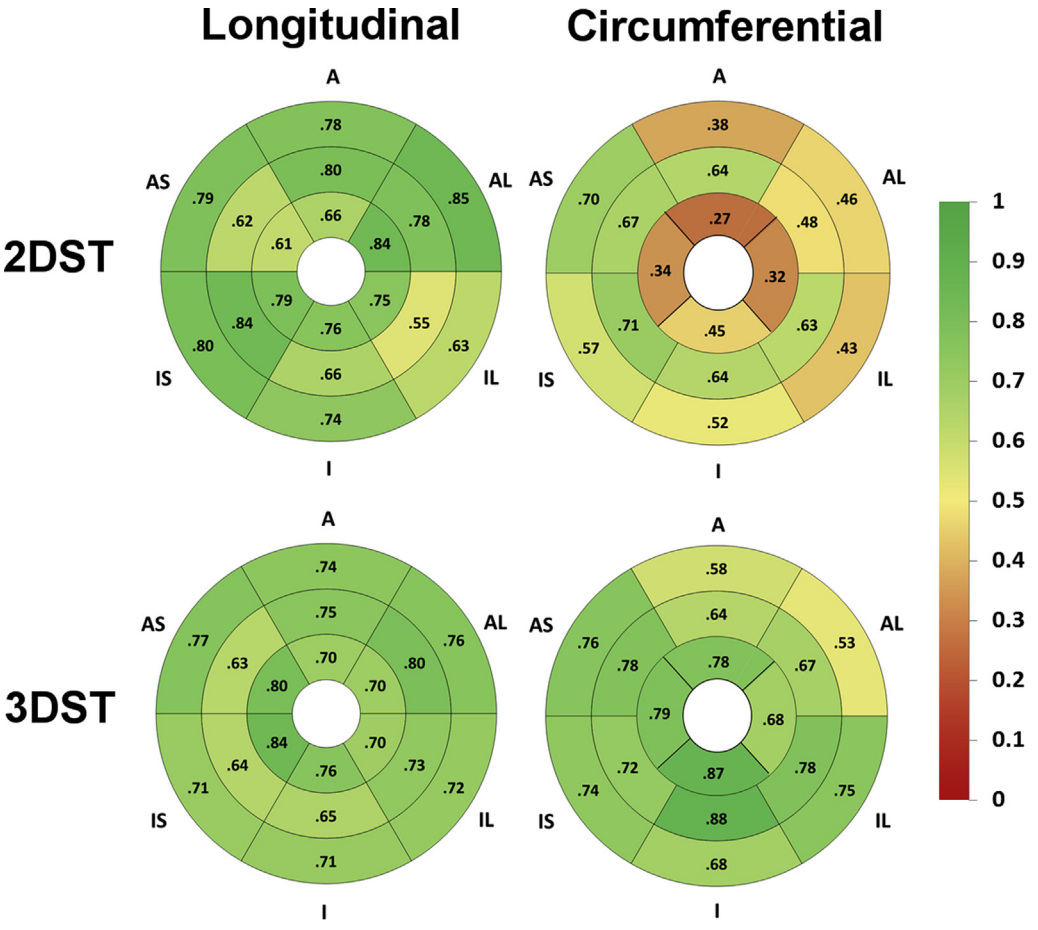

Figure 7 Test-rest reproducibility of segmental LS and CS by 2DST and 3DST. Values plotted in the bull's-eyes represent the mean ICC per segment. *A*, Anterior; *AL*, anterolateral; *AS*, anteroseptal; *I*, inferior; *IL*, inferolateral; *IS*, inferoseptal.

lower than previously reported in the literature,[23,24] although comparable with 2D tagging. Despite efforts toward standardization by the European Association of Cardiovascular Imaging in partnership with industry, part of the difference in normal strain values with the already published data probably arises from the large intervendor variability in the implemented 3DST algorithms, different regularization of strain curves, and varying postprocessing steps.[25]

Test-Retest Variability

The superior reproducibility of 3D over 2D echocardiography for LV volume and ejection fraction quantification has been thoroughly demonstrated.[26] Previous studies documenting strain measurement reproducibility have mainly assessed the intra- and interobserver variability of 3DST and 2DST[23] and less the test-retest reproducibility of 2DST techniques,[27] while very few studies so far have assessed the test-retest variability of 3DST.[28] Our study is therefore among the first to investigate any advantage of 3DST over 2DST by directly comparing the capabilities of the two methods. We found that the test-retest reproducibility of 3DST is comparable with that of 2DST for longitudinal global, regional, and segmental strain analysis, whereas it is superior to 2DST for CS assessment at all levels. Undoubtedly, this is due to the difficulty of reproducing the short-axis planes, especially at the apical level.[29]

Clinical Implications

Our study suggests that the assessment of LV deformation by 3DST could represent a further step toward understanding cardiac function, allowing more accurate and more reproducible assessment of global and regional deformation than 2DST. Currently its application is limited to research purposes only, as trained observers and experienced cardiology centers are prerequisites for adequate image acquisition and analysis. Certainly, the added value of assessing 3D deformation to characterize heart disease and maybe provide data on prognosis needs to be investigated in prospective clinical studies. Efforts from software developers should aim, besides standardization of 3D deformation estimates, at finding solutions to obtain accurate segmental strain information. It is reassuring, however, that by 3DST, reproducible data are obtained by different observers and promising as far as serial studies are concerned. Also, as 3DST and 2DST had similar test-retest reproducibility for LS measurement, 2DST-derived GLS, the parameter currently most investigated for deformation assessment, can continue to be used for follow-up studies in patients with different pathologies.

Limitations

We acknowledge several limitations of our study. First, in the absence of a gold standard for 3D deformation assessment, we considered 2D tagging as the frame of reference, as this is the current method thought to provide validated and accurate strain measurements. However, inaccuracy of the 2DTagg method itself could also potentially contribute to the observed strain differences.

Second, a nonnegligible factor is that the frame rates of 3DST and 2DTagg were lower than for 2DST, which could therefore lead to underestimation of deformation because of insufficient temporal resolution. Studies assessing the impact of frame rate on strain measurements have suggested that the comparison between 3DST and 2DST is not compromised at a temporal resolution of 18 to 25 frames/sec for the 3D data set.[30,31] Also, because current 3DST image quality is typically inferior to that of 2DST, in our study we used only good-quality 3D data sets, and therefore our results cannot be applied to real-life practice.

Last, but importantly, our results cannot be extrapolated to other vendors, as the study was not designed to investigate more than one software developer. Additionally, we compared the performance of 3DST and 2DST versus 2DTagg, however, as it is of recent development, we have not yet investigated the clinical additive value of 3DST. Further prospective studies are needed in order to address this question.

CONCLUSION

Our findings demonstrate the superiority of 3DST over 2DST for evaluation of global longitudinal and circumferential myocardial deformation compared with 2D cardiac magnetic resonance tagging. However, segmental deformation assessment was not significantly improved by 3DST analysis compared with 2DST, suggesting that both these techniques need further refinement in order to accurately characterize regional myocardial abnormalities.

ACKNOWLEDGMENT

We thank David Prater and his team at Philips Ultrasound for their support in this work. We would like to thank the echocardiography technicians from the Echo Lab of Cliniques Universitaires Saint Luc for their precious help with image acquisition for the test-retest reproducibility.

SUPPLEMENTARY DATA

Supplementary data related to this article can be found online at https://doi.org/10.1016/j.echo.2018.04.009.

REFERENCES

1. Collier P, Phelan D, Klein A. A test in context: myocardial strain measured by speckle-tracking echocardiography. J Am Coll Cardiol 2017;69:1043-56.
2. Geyer H, Caracciolo G, Abe H, Wilansky S, Carerj S, Gentile F, et al. Assessment of myocardial mechanics using speckle tracking echocardiography: fundamentals and clinical applications. J Am Soc Echocardiogr 2010;23:351-69.
3. Gorcsan J III, Tanaka H. Echocardiographic assessment of myocardial strain. J Am Coll Cardiol 2011;58:1401-13.
4. Kalam K, Otahal P, Marwick TH. Prognostic implications of global LV dysfunction: a systematic review and meta-analysis of global longitudinal strain and ejection fraction. Heart 2014;100:1673-80.
5. Amundsen BH, Helle-Valle T, Edvardsen T, Torp H, Crosby J, Lyseggen E, et al. Noninvasive myocardial strain measurement by speckle tracking echocardiography: validation against sonomicrometry and tagged magnetic resonance imaging. J Am Coll Cardiol 2006;47:789-93.
6. Korinek J, Wang J, Sengupta PP, Miyazaki C, Kjaergaard J, McMahon E, et al. Two-dimensional strain—a Doppler-independent ultrasound method for quantitation of regional deformation: validation in vitro and in vivo. J Am Soc Echocardiogr 2005;18:1247-53.
7. Farsalinos KE, Daraban AM, Unlu S, Thomas JD, Badano LP, Voigt JU. Head-to-head comparison of global longitudinal strain measurements among nine different vendors: the EACVI/ASE Inter-Vendor Comparison Study. J Am Soc Echocardiogr 2015;28:1171-81.e2.
8. Nagata Y, Takeuchi M, Mizukoshi K, Wu VC, Lin FC, Negishi K, et al. Intervendor variability of two-dimensional strain using vendor-specific and vendor-independent software. J Am Soc Echocardiogr 2015;28:630-41.
9. Risum N, Ali S, Olsen NT, Jons C, Khouri MG, Lauridsen TK, et al. Variability of global left ventricular deformation analysis using vendor dependent and independent two-dimensional speckle-tracking software in adults. J Am Soc Echocardiogr 2012;25:1195-203.
10. Voigt JU, Pedrizzetti G, Lysyansky P, Marwick TH, Houle H, Baumann R, et al. Definitions for a common standard for 2D speckle tracking echocardiography: consensus document of the EACVI/ASE/Industry Task Force

to Standardize Deformation Imaging. J Am Soc Echocardiogr 2015;28:183-93.

11. Amzulescu MS, Langet H, Saloux E, Manrique A, Boileau L, Slimani A, et al. Head-to-head comparison of global and regional two-dimensional speckle tracking strain versus cardiac magnetic resonance tagging in a multicenter validation study. Circ Cardiovasc Imaging 2017;10:e006530.
12. Seo Y, Ishizu T, Atsumi A, Kawamura R, Aonuma K. Three-dimensional speckle tracking echocardiography. Circ J 2014;78:1290-301.
13. Urbano-Moral JA, Patel AR, Maron MS, Arias-Godinez JA, Pandian NG. Three-dimensional speckle-tracking echocardiography: methodological aspects and clinical potential. Echocardiography 2012;29:997-1010.
14. Reant P, Labrousse L, Lafitte S, Bordachar P, Pillois X, Tariosse L, et al. Experimental validation of circumferential, longitudinal, and radial 2-dimensional strain during dobutamine stress echocardiography in ischemic conditions. J Am Coll Cardiol 2008;51:149-57.
15. Altman M, Bergerot C, Aussoleil A, Davidsen ES, Sibellas F, Ovize M, et al. Assessment of left ventricular systolic function by deformation imaging derived from speckle tracking: a comparison between 2D and 3D echo modalities. Eur Heart J Cardiovasc Imaging 2014;15:316-23.
16. Saito K, Okura H, Watanabe N, Hayashida A, Obase K, Imai K, et al. Comprehensive evaluation of left ventricular strain using speckle tracking echocardiography in normal adults: comparison of three-dimensional and two-dimensional approaches. J Am Soc Echocardiogr 2009;22:1025-30.
17. Obokata M, Nagata Y, Wu VC, Kado Y, Kurabayashi M, Otsuji Y, et al. Direct comparison of cardiac magnetic resonance feature tracking and 2D/3D echocardiography speckle tracking for evaluation of global left ventricular strain. Eur Heart J Cardiovasc Imaging 2016;17:525-32.
18. Somphone O, Craene MD, Ardon R, Mory B, Allain P, Gao H, et al. Fast myocardial motion and strain estimation in 3D cardiac ultrasound with Sparse Demons. Presented at: 2013 IEEE 10th International Symposium on Biomedical Imaging; San Francisco, CA; July 15, 2013.
19. Tsang W, Salgo IS, Medvedofsky D, Takeuchi M, Prater D, Weinert L, et al. Transthoracic 3D echocardiographic left heart chamber quantification using an automated adaptive analytics algorithm. JACC Cardiovasc Imaging 2016;9:769-82.
20. Seo Y, Ishizu T, Enomoto Y, Sugimori H, Yamamoto M, Machino T, et al. Validation of 3-dimensional speckle tracking imaging to quantify regional myocardial deformation. Circ Cardiovasc Imaging 2009;2:451-9.
21. Heyde B, Bouchez S, Thieren S, Vandenheuvel M, Jasaityte R, Barbosa D, et al. Elastic image registration to quantify 3-D regional myocardial deformation from volumetric ultrasound: experimental validation in an animal model. Ultrasound Med Biol 2013;39:1688-97.
22. Mirea O, Pagourelias ED, Duchenne J, Bogaert J, Thomas JD, Badano LP, et al. Intervendor differences in the accuracy of detecting regional functional abnormalities: a report from the EACVI-ASE Strain Standardization Task Force. JACC Cardiovasc Imaging 2018;11:25-34.
23. Muraru D, Cucchini U, Mihaila S, Miglioranza MH, Aruta P, Cavalli G, et al. Left ventricular myocardial strain by three-dimensional speckle-tracking echocardiography in healthy subjects: reference values and analysis of their physiologic and technical determinants. J Am Soc Echocardiogr 2014;27:858-71.e1.
24. Kleijn SA, Pandian NG, Thomas JD, Perez de Isla L, Kamp O, Zuber M, et al. Normal reference values of left ventricular strain using three-dimensional speckle tracking echocardiography: results from a multicentre study. Eur Heart J Cardiovasc Imaging 2015;16:410-6.
25. Jasaityte R, Heyde B, D'Hooge J. Current state of three-dimensional myocardial strain estimation using echocardiography. J Am Soc Echocardiogr 2013;26:15-28.
26. Jenkins C, Bricknell K, Hanekom L, Marwick TH. Reproducibility and accuracy of echocardiographic measurements of left ventricular parameters using real-time three-dimensional echocardiography. J Am Coll Cardiol 2004;44:878-86.
27. Mirea O, Pagourelias ED, Duchenne J, Bogaert J, Thomas JD, Badano LP, et al. Variability and reproducibility of segmental longitudinal strain measurement: a report from the EACVI-ASE Strain Standardization Task Force. JACC Cardiovasc Imaging 2018;11:15-24.
28. Badano LP, Cucchini U, Muraru D, Al Nono O, Sarais C, Iliceto S. Use of three-dimensional speckle tracking to assess left ventricular myocardial mechanics: inter-vendor consistency and reproducibility of strain measurements. Eur Heart J Cardiovasc Imaging 2013;14:285-93.
29. Goffinet C, Chenot F, Robert A, Pouleur AC, le Polain de Waroux JB, Vancrayenest D, et al. Assessment of subendocardial vs. subepicardial left ventricular rotation and twist using two-dimensional speckle tracking echocardiography: comparison with tagged cardiac magnetic resonance. Eur Heart J 2009;30:608-17.
30. Yodwut C, Weinert L, Klas B, Lang RM, Mor-Avi V. Effects of frame rate on three-dimensional speckle-tracking-based measurements of myocardial deformation. J Am Soc Echocardiogr 2012;25:978-85.
31. Rosner A, Barbosa D, Aarsaether E, Kjonas D, Schirmer H, D'Hooge J. The influence of frame rate on two-dimensional speckle-tracking strain measurements: a study on silico-simulated models and images recorded in patients. Eur Heart J Cardiovasc Imaging 2015;16:1137-47.

Supplemental Table 1 GLS and GCS stratified by technique in healthy volunteers and patients with LV dysfunction and hypertrophy

Strain	Technique	Volunteers (n = 29)	Dysfunction (n = 63)	Hypertrophy (n = 27)	P
GLS (%)	2DST	−21 ± 2*	−14 ± 5†	−17 ± 4	<.001
	3DST	−14 ± 2*	−9 ± 3†	−11 ± 3	<.001
	2DTagg	−15 ± 2*	−9 ± 4†	−11 ± 3	<.001
GCS (%)	2DST	−26 ± 4*	−13 ± 6†	−23 ± 5	<.001
	3DST	−15 ± 2	−9 ± 3†	−14 ± 4	<.001
	2DTagg	−16 ± 2*	−10 ± 3†	−13 ± 1	<.001

Data are expressed as mean ± SD.
*P < .001 versus dysfunction and hypertrophy.
†P < .01 versus volunteers and hypertrophy.